ASIIMETRIK
JURNAL ILMIAH REKAYASA DAN INOVASI
p-ISSN: 2655-1861, **e-ISSN:** 2716-2923
Volume **8** Number **1**, **2026**

Effect of Oil Viscosity as a Quenching Medium on Hardness and Corrosion Rate of Mild Steel After Hardfacing

Muhammad Fatihuddin[1*], Reza Febriano Armas[1], Ferry Budhi Susetyo[1], Syamsuir[1], Basori[2], Muhammad Yunan Hasbi[3]
[1]Department of Mechanical Engineering, Universitas Negeri Jakarta, Jakarta, Indonesia
[2]Department of Mechanical Engineering, Universitas Nasional, Jakarta, Indonesia
[3]Research Center for Metallurgy-National Research and Innovation Agency, Tangerang Selatan, Indonesia

***Correspondence email**: *mfatihuddin@unj.ac.id*

Received: 22/11/2025 Revised: 27/12/2025 Accepted: 06/01/2026

Abstract: This study investigates the effect of oil viscosity as a quenching medium on the hardness and corrosion rate of mild steel after hardfacing. The specimens were quenched using oils of different viscosities (SAE 30, SAE 40, and SAE 50) after hardfacing treatment. Microstructural analysis using an Olympus BX51M optical microscope revealed that lower-viscosity oil produced a more dominant martensitic phase, while higher-viscosity oils resulted in greater formation of ferrite and pearlite due to slower cooling rates. The Vickers hardness test showed the highest hardness value of 460.44 VHN for SAE 30, decreasing to 415.18 VHN for SAE 50. Electrochemical testing indicated that the corrosion current density (Icorr) and corrosion rate increased with oil viscosity, from 95.2 µA/cm² and 1.114 mmpy (SAE 30) to 129.1 µA/cm² and 1.511 mmpy (SAE 50). The results demonstrate that lower-viscosity oils enhance martensitic transformation, improve hardness, and reduce corrosion rate, highlighting viscosity control as a key factor in optimizing post-hardfacing heat treatment performance.

Keywords: oil; viscosity; quenching; hardness; corrosion

SDGs Problem Solving

The research on oil viscosity as a quenching medium for hardfacing mild steel strongly corresponds with SDGs Chapter #9. It optimizes material performance through experimental research and problem-solving, increases durability, mitigates corrosion-related losses, and fosters sustainable industrial innovation and efficient engineering methods.

1. INTRODUCTION

The quenching process is one of the most critical stages in the heat treatment of steel, as it transforms austenite into harder phases such as martensite, directly influencing the mechanical and electrochemical properties of the material. The selection of an appropriate quenching medium determines the cooling rate, phase composition, and consequently, the final properties of the steel (Patil *et al.*, 2023).

The selection of cooling media in the quenching process must be carried out carefully, as it greatly influences the quality of the heat-treatment results. Commonly used media include water, oil, salt water solutions, and coolant (Sopiyan, Basori and Susetyo, 2020). Various studies report that each medium produces different hardness levels. However, water is often considered superior because it provides good hardness improvement and is abundantly available in nature . For medium-carbon steel, hardness can increase more significantly when quenching is performed using ice water after heat treatment.

Among various quenching media, oil is widely used due to its ability to provide controlled cooling, minimize distortion, and reduce the risk of cracking compared to water or brine quenching. One of the most important parameters of quenching oil is its viscosity, which significantly affects the heat transfer capability during the cooling process (Hájek, Dlouha and Průcha, 2021).

The rate of heat extraction during quenching is strongly influenced by oil viscosity. Oils with lower viscosity promote faster heat transfer, resulting in a higher cooling rate and enhanced formation of martensitic phases with greater hardness (Laxmi *et al.*, 2022, 2024). Conversely, oils with higher viscosity reduce the cooling rate, allowing diffusion-controlled transformations that lead to the formation of ferrite and pearlite phases.

These softer microstructures contribute to lower hardness values (Ejiko, Fatona and Ibikunle, 2024). Similar findings were reported , who observed that fast-cooling oils produced finer pearlitic and martensitic structures, whereas high-viscosity oils tended to form coarser ferrite–pearlite mixtures (Syaripuddin *et al.*, 2025). These microstructural changes directly contribute to an increase in the material's hardness by altering the internal arrangement and characteristics of its constituent phases (Syamsuir *et al.*, 2023).

In addition to influencing hardness, the cooling rate and the resulting microstructure significantly affect the corrosion behavior of steel (Ishtiaq *et al.*, 2022). The martensitic structure formed under rapid cooling conditions generally exhibits a finer and more uniform morphology, minimizing the formation of micro-galvanic cells and reducing the corrosion current density (Icorr) (Jo *et al.*, 2020). Therefore, controlling the viscosity of quenching oil is a crucial factor in achieving an optimal balance between hardness and corrosion resistance in mild steel after hardfacing (Susetyo, Kholil and Fatihuddin, 2019).

This research aims to systematically evaluate the influence of oil viscosity as a quenching medium on the hardness and corrosion rate of mild steel subjected to a hardfacing process. Three different oil viscosities SAE 30, SAE 40, and SAE 50, were employed to examine their effects on the cooling rate, microstructural evolution, mechanical properties, and electrochemical behavior of the material.

The analysis of these interrelated parameters provides a comprehensive understanding of the role of quenchant viscosity in post-hardfacing heat treatment, contributing to the optimization of steel performance and corrosion resistance for industrial applications.

2. METHODOLOGY

This study employed an experimental method consisting of material preparation, hardfacing and quenching, microstructural observation, hardness testing, and electrochemical corrosion analysis.

2.1. Material

The material used in this study was low-carbon steel containing 0.2% carbon, with dimensions of 150 × 10 × 10 mm, as illustrated in Figure 1. And Engine oils with different viscosities are SAE 10W-30, SAE 10W-40, and SAE 20W-50 were used as quenching media. Viscosity directly affects the cooling rate during quenching, which ultimately determines the final material properties after heat treatment, such as hardness and microstructure. Previous studies have also demonstrated that variations in quenchant viscosity lead to significant differences in the hardness after quenching (Laxmi *et al.*, 2022).

Figure 1. Mild Steel 150 x 10 x 10 mm

2.2. Heat Treatment

The hardfacing process was using a surface welding technique with an HV450 electrode of 3.2 mm diameter and a current of 110 A. The specimens were then direct quenched in cooling media with variously oil viscosities, namely SAE 30, SAE 40, and SAE 50. Figure 2 shows the welded specimens that were directly quenched in oil quenching media with different viscosities.

(a). Directly quenched in various of oils

(b). The quenched specimen

Figure 2. The welded and directly quenched specimen

2.3. Microstructure

The quenched specimens were then cut and polished using sandpaper up to a grit size of #5000, to drying. Then, the specimens were etched using Nital, drying again. After the etching process, the specimens were observed using an optical microscope (Olympus BX51M) to obtain the microstructure.

2.4. Testing Methode

A Vickers hardness tester, Future Tech (FV 300e), was used to do the hardness test in this study, as shown in Figure 3a. The average of these measurements was used to find the hardness value. Figure 3b shows where five repeated indentation spots were tested with a force of 5 kg.

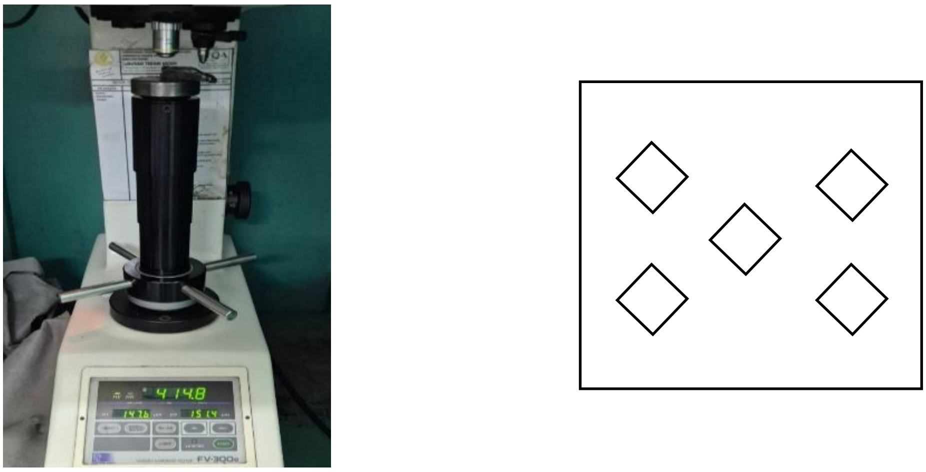

(a). Vickers Hardness machine (b). Indentation points

Figure 3. Testing method

The electrochemical test was conducted using a Potentiodynamic system in a 3.5% NaCl solution. The specimen was used as the working electrode, platinum wire as the counter electrode, and Ag/AgCl as the reference electrode. The electrochemical measurement employed the linear sweep voltammetry (LSV) method, conducted at a scan rate of 5 mV/s within the potential range of −1.2 to −0.8 V vs. Ag/AgCl. The Tafel extrapolation was performed from the LSV curve to determine the corrosion potential and corrosion current. From the LSV curve, Tafel extrapolation was performed to determine the corrosion current and potential. The corrosion rate was then calculated using Faraday's equation (Manik, Chrismianto and Prayoga, 2023):

$$CR = \frac{K \times Icorr \times EW}{\rho} \quad (1)$$

where CR is corrosion rate in(mm/year); K is conversion constant; Icorr is corrosion current in ($\mu A/cm^2$); EW is equivalent weight of the metal; and ρ is metal density (g/cm^3). Ossila potentiostat was used for OCP and LSV investigation. The investigations were conducted in 3.5% NaCl at room temperature.

3. RESULTS AND DISCUSSION

3.1. Microstructure

Microstructure observation was conducted by Olympus BX51M optical microscope. Figure 4 shows that variations in oil viscosity influence the cooling rate and the type of phases formed during the quenching process. In the specimen quenched with SAE 30 oil, the formation of martensite was more dominant compared to those quenched with SAE 40 and SAE 50 oils.

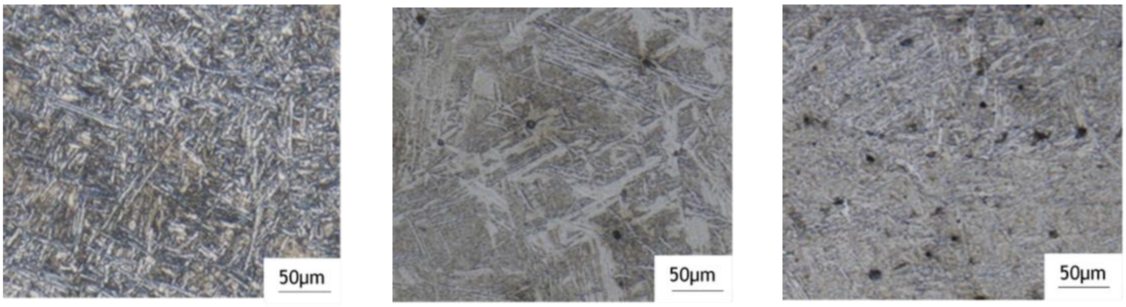

(a). SAE 30 (b). SAE 40 (c). SAE 50

Figure 4. Microstructure of various oil viscosity

The specimen quenched with SAE 30 oil (Figure 4a) exhibits a microstructure mostly characterized by tiny, needle-like and lath-shaped features typical of martensite. The comparatively reduced viscosity of SAE 30 oil facilitates a more rapid cooling rate by enhancing heat dissipation from the heated specimen. Rapid cooling inhibits diffusional transformations like pearlite or bainite production, instead promoting the diffusion less transition of austenite into martensite. Consequently, the microstructure exhibits a more refined and tightly packed arrangement of martensitic laths. This refined martensitic structure often associates with increased hardness and strength owing to the elevated dislocation density and carbon supersaturation in the martensite phase.

Conversely, the specimen quenched with SAE 40 oil (Figure 4b) has a much less homogeneous martensitic structure. The heightened viscosity of SAE 40 diminishes the cooling rate compared to SAE 30. Gradual heat extraction permits restricted diffusional processes to transpire before to the completion of the martensitic transformation. As a result, minor patches of bainite or residual austenite may develop in conjunction with martensite. The microstructure has a coarser appearance, characterized by fewer well defined lath boundaries. This indicates a partial decrease in the martensitic proportion relative to the SAE 30-quenched specimen.

The specimen quenched with SAE 50 oil (Figure 4c) demonstrates the most significant divergence from a completely martensitic structure. SAE 50 oil, owing to its elevated viscosity, offers the most sluggish cooling rate of the three mediums. The gradual quenching diminishes the extent of undercooling, facilitating enhanced diffusion of carbon atoms and encouraging the development of non-martensitic phases like bainite or fine pearlite in certain areas. Darker spots may signify the presence of carbides, residual austenite, or transformation products resulting from delayed cooling. The martensite proportion is noticeably reduced, and the structure exhibits greater heterogeneity.

This is attributed to the faster cooling rate in the low viscosity oil, which promotes a more complete transformation of austenite into martensite (Syamsuir *et al.*, 2024). However, the specimen quenched with SAE 50 oil exhibited a microstructure containing a greater amount of ferrite and pearlite phases, indicating a slower cooling process (Susetyo, Kholil and Fatihuddin, 2019).

Oils with higher viscosity can reduce the cooling rate during the quenching process, thereby limiting the extent of martensitic transformation. Consequently, the resulting microstructure contains a lower martensitic phase and a higher proportion of diffusion-controlled phases (Wibowo *et al.*, 2025).

3.2. Hardness Test Results

The hardness test conducted using the Vickers method. Table 1 shows the Vickers Hardness Number (VHN) results for three different SAE steel grades: SAE 30, SAE 40, and SAE 50. Five indentation measurements (A–E) were taken for each grade to check how consistent and reproducible the hardness data was. This led to the average hardness being calculated.

Table 1. Vickers Hardness Number (VHN)

SAE	Indentation Points (VHN)					Avg. (VHN)
	A	B	C	D	E	
30	461.7	461.1	459.8	459.5	460.1	460.44
40	435.2	434.2	434.6	435.5	434.2	434.97
50	415.5	415.7	417.3	413.1	414.8	415.18

The VHN values for SAE 30 range from 459.5 to 461.7. The difference between the highest and lowest values is only 2.2 VHN, which shows that the measurements are very consistent. The average hardness of SAE 30 is 460.44 VHN. The higher hardness value means that SAE 30 is less likely to bend than the other two classes in this dataset. The small changes in the data suggest that the microstructure is stable and the testing conditions are stable.

The hardness ratings for SAE 40 range from 434.2 VHN to 435.5 VHN. The difference of only 1.3 VHN between the highest and lowest measurements shows that this is more consistent than SAE 30. The average hardness that was calculated is 434.97 VHN. SAE 40 is a little softer than SAE 30, with a hardness difference of about 25 VHN. This decrease could be due to changes in composition, heat treatment, or carbon content, depending on how the material is being processed.

The indentation results for SAE 50 are between 413.1 VHN and 417.3 VHN, which is a difference of 4.2 VHN. This change, which is slightly bigger than the other two classes, is small enough to show that the tests can be repeated. The mean hardness value of 415.18 VHN is the lowest of the three materials tested. The steady drop in hardness from SAE 30 to SAE 50 shows that the qualities of the materials are changing in a systematic way, which could be due to microstructural phases or the way they were heated.

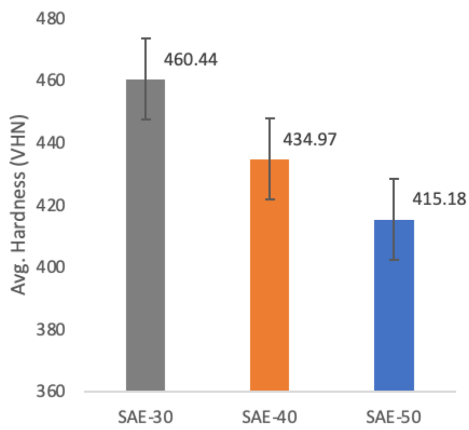

Figure 5. Average of Hardness of various oil viscosity

Figure 5 shows the average hardness values (in Vickers Hardness Number, VHN) for samples tested with three different oil viscosities: SAE-30, SAE-40, and SAE-50. The data clearly shows that the hardness goes down as the oil viscosity goes from SAE-30 to SAE-50.

SAE-30 has the highest average hardness, at 460.44 VHN. This means that the sample that was treated or quenched with SAE-30 oil had the highest resistance to indentation, which means that the hardening process worked better. SAE-30 has a higher hardness value than other viscosities, which means it cools faster. This helps make harder microstructures, like martensite, during heat treatment. The average hardness of SAE-40 goes down to 434.97 VHN. This is a big drop compared to SAE-30. The moderate hardness value shows that SAE-40 oil doesn't cool as well as it could because it is more viscous. An oil with a high viscosity usually makes it harder to remove heat during quenching, which slows down the cooling process. Because of this, the microstructure may have fewer hard phases, which will make it less hard overall. SAE-50 has a minimum hardness value of 415.18 VHN. This further reduction supports the idea that thicker oil makes quenching less effective. SAE-50 is the most viscous of the three oils, so it probably cools the slowest. When cooling is slower, it can allow some parts to change to softer phases like bainite or pearlite, which makes the material less hard.

The error bars in the picture show how much the measurements can change or how much they can vary. There is some overlap between the error ranges, but the basic trend of decreasing stays the same. The error bars show that the hardness tests do have some natural variation, but the differences between the three oil viscosities are not random; they are systematic.

Figure 5 shows the specimen quenched in SAE 30 oil (the lowest viscosity) exhibited the highest hardness value is 460.44 VHN, followed by 434.97 VHN for SAE 40, and 415.18 VHN for SAE 50. The hardness value of a material can become higher after quenching (Susetyo, Basori and Maryanto, 2020). The reduction in hardness with increasing oil viscosity can be attributed to the decrease in cooling rate, which limits the formation of martensite during quenching (Amosun *et al.*, 2022). A slower cooling process allows for the diffusion of carbon atoms, leading to the development of softer microstructure constituents such as ferrite and pearlite instead of martensite (Wang *et al.*, 2021).

Quenching oils with higher viscosity exhibit a lower cooling rate, which leads to a reduced formation of martensite and consequently lower hardness values (Zhang *et al.*, 2022). Therefore, the results of this study confirm that oils with lower viscosity enhance the cooling rate, promote a more complete transformation of austenite into martensite, and consequently result in higher hardness values.

3.3. Corrosion

Figure 6 shown the Open Circuit Potential (OCP) test results, offering a comparative analysis of the corrosion resistance of metallic samples submerged in a 3.5% NaCl solution, safeguarded by three distinct grades of engine oil: SAE 30, SAE 40, and SAE 50, over a duration of 1200 seconds. The Open Circuit Potential (OCP) is a critical electrochemical test that indicates a metal's thermodynamic inclination to corrode in a certain environment, without external current, with larger negative potentials often signifying an increased likelihood of corrosion.

In this experiment, the open circuit potential (OCP) values for samples treated with SAE 30, SAE 40, and SAE 50 oils were measured using an Ag/AgCl reference electrode, yielding steady-state values of -0.59 V, -0.58 V, and -0.55 V, respectively, after 1200 seconds. The OCP curves exhibit a swift initial decline in potential, characteristic of the metal surface experiencing rapid electrochemical reactions, including chloride ion adsorption, initial oxide formation, and reorganization of the double layer at the metal-electrolyte interface. This abrupt decline is succeeded by a prolonged stabilization phase in which the surface attains a quasi-equilibrium condition, indicating a balance between the anodic and cathodic reactions that regulate corrosion processes (Mihajlović *et al.*, 2017).

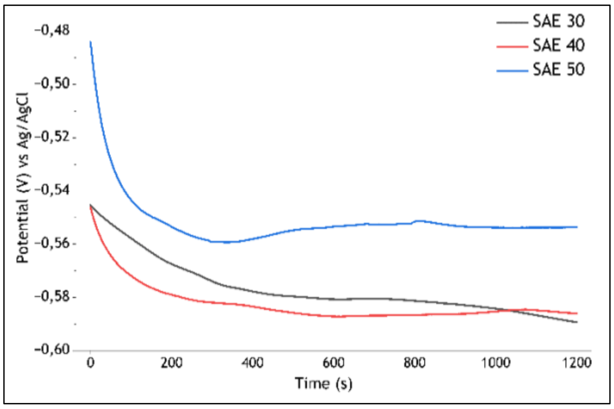

Figure 6. OCP result

The data unequivocally indicates that SAE 50 oil offers superior corrosion protection, as seen by its minimal negative OCP value, implying a reduced thermodynamic impetus for metal dissolution relative to the other oils. The enhanced performance is due to the physical and chemical characteristics of SAE 50, particularly its elevated viscosity, which facilitates the formation of a stronger and more uniform oil film on the metal surface, serving as a more efficient barrier against the intrusion of aggressive chloride ions from the saline solution. Conversely, SAE 30, exhibiting the most negative OCP, signifies a thinner and perhaps less adherent protective layer, resulting in less resistance to electrolyte infiltration and hence increased corrosion vulnerability. SAE 40 demonstrates intermediate properties, according to its viscosity and protective attributes that lie between those of SAE 30 and SAE 50. The diverse behaviors exhibited by the oils presumably arise from differences in layer thickness, stability, and potential interactions with the metal surface, all of which affect the degree to which the oil might hinder electrochemical processes that facilitate corrosion.

Moreover, the use of a 3.5% NaCl solution is especially pertinent as it closely replicates maritime conditions, creating a highly corrosive environment that highlights the disparities in protective efficacy among the oil grades. These findings have substantial consequences for the choosing of lubricants or protective coatings in settings where corrosion significantly threatens metal integrity, such as maritime, coastal, or industrial applications.

The capacity of higher viscosity oils, such as SAE 50, to provide enhanced protection may warrant their use in certain contexts, notwithstanding some compromises in lubrication and mechanical efficiency. The OCP results in Figure 6 emphasize the significance of oil viscosity and film-forming capability in reducing corrosion, indicating that even minor enhancements in these characteristics can lead to considerable improvements in the durability and dependability of metallic components subjected to severe saline conditions.

The results show that the oxide layer on the upper surface of the sample easily detaches and dissolves into the solution . The sample quenched in SAE 30 oil shifts toward more negative potentials and reaches a stable condition after approximately 1200 seconds of testing. Meanwhile, the samples quenched in SAE 40 and SAE 50 remain in a stable condition from 400 to 1200 seconds of measurement.

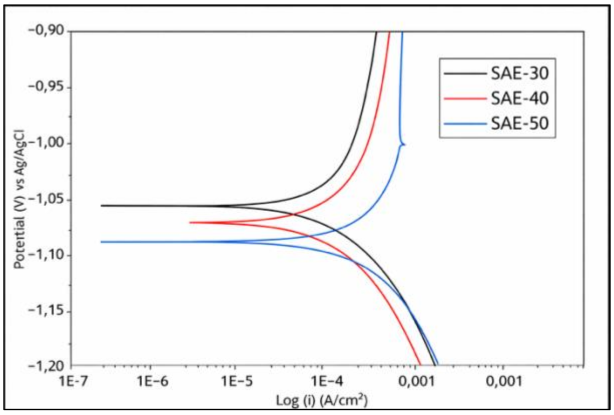

Figure 7. Polarization curve of various oil viscosity

Figure 7 shows the potentiodynamic polarization curves of mild steel samples that were quenched in SAE 30, SAE 40, and SAE 50 oils and then tested in a 3.5% NaCl solution. This shows how each condition reacts to corrosion in a chloride-rich environment that simulates exposure to seawater. The polarization curves show the potential (V vs Ag/AgCl) on the vertical axis and the logarithm of current density (log i, A/cm²) on the horizontal axis. This makes it easier to figure out important corrosion parameters like corrosion potential, corrosion current density (Icorr), and anodic-cathodic kinetics. The corrosion potentials for the three samples are around −1.05 to −1.10 V versus Ag/AgCl. The SAE 30-quenched sample has a slightly more noble (less negative) than the SAE 40 and SAE 50 samples. This change toward a better outcome shows that steel quenched in SAE 30 oil is less likely to corrode in a 3.5% NaCl solution. On the other hand, the SAE 50 sample has a stronger negative, which means that it is more likely to start corroding under the same testing conditions. The polarization curves show changes in corrosion current density, which is directly related to the corrosion rate.

The convergence of the extrapolated anodic and cathodic Tafel areas indicates that SAE 30 generally has a lower corrosion current density than SAE 40 and SAE 50, which means it is more resistant to corrosion. The cathodic branches, primarily associated with oxygen reduction in aerated NaCl solution, display similar slopes across the three samples, suggesting that the cathodic reaction mechanism remains uniform regardless of the quenching medium. However, differences in the anodic branches are more obvious, which could mean that the iron dissolving behaviour is different because the microstructure changes when the oil viscosity changes during quenching. SAE 30 oil has a lower viscosity, which makes it cool down faster than SAE 40 and SAE 50. This increases the amount of martensitic structure and makes the microstructural features finer. This optimized microstructure can make things harder and lower the rate at which anodic cells form between phases, which slows down the rate at which anodic cells dissolve. Higher viscosity oils, like SAE 50, cool down more slowly. This can cause a mixed microstructure with more ferrite–pearlite or coarser martensite, which can speed up corrosion by increasing micro-galvanic activity. The anodic curves in the high current density zone show a sharp rise in potential, which means that active dissolution is happening without a clear passive region. This is typical of mild steel in environments with high chloride levels, where it is hard to keep stable passive films. The absence of a broad passive plateau signifies that chloride ions continuously destabilize any developing oxide layer, leading to persistent metal dissolution. The small differences in Tafel slopes between the samples show that the charge transfer resistance and surface reactivity are different, which supports the idea that the viscosity of the quenching media affects the electrochemical response.

The polarization behaviour shows that the choice of quenching oil has a big effect on the mechanical properties and corrosion resistance of mild steel in salty water. In the situations that were looked at, SAE 30-quenched steel had the best corrosion properties, followed by SAE 40. SAE 50, on the other hand, was a little more prone to corrosion. The results show that the parameters used for heat treatment, the resulting microstructure, and the electrochemical stability in harsh chloride environments are all closely related. This means that it is important to choose the right quenching medium to make mild steel parts stronger and last longer in marine or coastal conditions.

The specimen quenched in SAE 30 exhibits the lowest corrosion current density, indicating superior corrosion resistance, while higher oil viscosity results in increased corrosion current density due to slower cooling rates and the formation of less uniform microstructures.

Table 2. Corrosion rate values

No.	SAE	Icorr (µA/Cm2)	Ecorr (mV)	Corrosion rate (mmpy)
1.	30	95.2	-1055.4	1.114
2.	40	114.4	-1069.5	1.338
3.	50	129.1	-1088.2	1.511

Based on the electrochemical tests, the corrosion current density (Icorr) and corrosion rate increased with the viscosity of the quenching oil (Jo *et al.*, 2020). As shown in Table 2, the Icorr value increase from 95.2 µA/cm² for the specimen quenched in SAE 30 oil to 129.1 µA/cm² in SAE 50 oil, while the corrosion rate increased from 1.114 mmpy to 1.511 mmpy.

This trend indicates that higher viscosity oils provide a slower cooling rate, resulting in a lower fraction of martensite and greater formation of ferrite and pearlite phases, which are electrochemically heterogeneous (Nnoka, Alaso Jack and Szpunar, 2024). However, the martensitic structure formed during rapid cooling exhibits a finer and more uniform morphology, which ultimately contributes to the reduction of corrosion current density (Tajmiri, Haider and Shabib, 2024).

4. CONCLUSION

The results of this study indicate that the viscosity of the quenching oil significantly influences the cooling rate, microstructure evolution, hardness, and corrosion behavior of mild steel after the hardfacing process. Microstructure analysis shown that specimens quenched in low viscosity oil (SAE 30) exhibited a more dominant martensitic structure due to a faster cooling rate, resulting in the highest hardness value. In contrast, specimens quenched in higher viscosity oils (SAE 40 and SAE 50) developed microstructures with greater fractions of ferrite and pearlite, indicating a slower cooling rate during the quenching process. This slower cooling promotes the formation of electrochemically heterogeneous phases and can increasing the corrosion rate

ACKNOWLEDGMENTS

The authors would like to thank the Faculty of Engineering, Universitas Negeri Jakarta and the National Research and Innovation Agency (BRIN), Indonesia, for their support in this research.

REFERENCES

Amosun, T.S. *et al.* (2022) 'Effect of quenching media on mechanical properties of welded mild steel plate'., *Mechanical Engineering for Society and Industry (MESI),* 3(1), pp. 3-11. Available at: https://doi.org/10.31603/mesi.7121.

Ejiko, S.O., Fatona, A.S. and Ibikunle, R.A. (2024) 'Investigation of Quenching on Microstructure and Mechanical Properties of Mild Steel', *IOSR Journal of Engineering (IOSRJEN)*, 14(4), pp. 29–38.

Hájek, J., Dlouha, Z. and Průcha, V. (2021) 'Comparison of Industrial Quenching Oils', *Metals*, 11(2), p. 250. Available at: https://doi.org/10.3390/met11020250.

Ishtiaq, M. *et al.* (2022) 'Microstructural, mechanical, and electrochemical analysis of carbon doped AISI carbon steels', *Applied Microscopy*, 52(1), p. 10. Available at: https://doi.org/10.1186/s42649-022-00079-w.

Jo, H. *et al.* (2020) 'Effects of Cooling Rate during Quenching and Tempering Conditions on Microstructures and Mechanical Properties of Carbon Steel Flange', *Materials*, 13(18), p. 4186. Available at: https://doi.org/10.3390/ma13184186.

Laxmi, B. *et al.* (2022) 'Quenchant oil viscosity and tempering temperature effect on mechanical properties of 42CrMo4 steel', *Journal of Materials Research and Technology*, 16, pp. 581–587. Available at: https://doi.org/10.1016/j.jmrt.2021.11.152.

Laxmi, B. *et al.* (2024) 'Austenitising temperature and quenchant viscosity influence on mechanical properties of normalised green oil quenched 42CrMo4 steel', *Cogent Engineering*, 11(1), p. 2340676. Available at: https://doi.org/10.1080/23311916.2024.2340676.

Manik, P., Chrismianto, D. and Prayoga, P.F. (2023) 'The Influence of SMAW Welding Current Variation on Tensile Strength, Corrosion Rate, and Microstructure of ST 42 Steel for Inner Bottom Plate Material in Ships', *International Journal of Marine Engineering Innovation and Research*, 8(2), pp. 279–288.

Mihajlović, M.B.P. *et al.* (2017) 'Imidazole based compounds as copper corrosion inhibitors in seawater', *Journal of Molecular Liquids*, 225, pp. 127–136. Available at: https://doi.org/10.1016/j.molliq.2016.11.038.

Nnoka, M., Alaso Jack, T. and Szpunar, J. (2024) 'Effects of different microstructural parameters on the corrosion and cracking resistance of pipeline steels: A review', *Engineering Failure Analysis*, 159, p. 108065. Available at: https://doi.org/10.1016/j.engfailanal.2024.108065.

Patil, J.P. *et al.* (2023) 'A Review on Effect of Different Quenching Media on Properties of Steel', *International Research Journal of Modernization in Engineering Technology and Science*, 5(5), pp. 6003–6008. Available at: https://doi.org/10.56726/IRJMETS39954.

Sopiyan, S., Basori, B. and Susetyo, F.B. (2020) 'The Effect of Water Temperature as Quenching Media on The Characteristics of HV 350 Weld Deposits', *SINTEK JURNAL: Jurnal Ilmiah Teknik Mesin*, 14(2), pp. 118–122. Available at: https://doi.org/10.24853/sintek.14.2.118-122.

Susetyo, F.B., Basori, I. and Maryanto, D. (2020) 'Pengaruh Direct dan In-Direct Quenching Dengan Media Air Terhadap Kekerasan Hasil Hardfacing Baja Karbon', *Jurnal Asiimetrik: Jurnal Ilmiah Rekayasa Dan Inovasi*, 2(2), pp. 125–131. Available at: https://doi.org/10.35814/asiimetrik.v2i2.1445.

Susetyo, F.B., Kholil, A. and Fatihuddin, M. (2019) 'Efek Polaritas Dan Media Pendingin Terhadap Nilai Kekerasan Permukaan Hardfacing Baja Karbon Rendah', *Jurnal Konversi Energi dan Manufaktur*, 6(1), pp. 1–5. Available at: https://doi.org/10.21009/JKEM.6.1.1.

Syamsuir *et al.* (2024) 'Spinning Effect of Barreling Plating on Physical Properties and Electrochemical Behavior of Copper Layers', *e-Journal of Surface Science and Nanotechnology*, 22(2), pp. 120–128. Available at: https://doi.org/10.1380/ejssnt.2024-003.

Syamsuir, S. *et al.* (2023) 'Rotating-Magnetic-Field-Assisted Electrodeposition of Copper for Ambulance Medical Equipment', *Automotive Experiences*, 6(2), pp. 290–302. Available at: https://doi.org/10.31603/ae.9067.

Syaripuddin *et al.* (2025) 'Different Quenching Media Effect on Microstructure, Hardness,and Corrosion of Medium Carbon Steel', *Jurnal Asiimetrik: Jurnal Ilmiah Rekayasa Dan Inovasi*, 7(2), pp. 219–226. Available at: https://doi.org/10.35814/asiimetrik.v7i2.8793.

Tajmiri, S., Haider, W. and Shabib, I. (2024) 'Effect of Heating Rate on Microstructure and Corrosion Resistance of Quenched and Tempered 8620 Low Carbon Alloy Steel', *Corrosion and Materials Degradation*, 5(3), pp. 370–386. Available at: https://doi.org/10.3390/cmd5030016.

Wang, H. *et al.* (2021) 'Effect of cooling rate on the microstructure and mechanical properties of a low-carbon low-alloyed steel', *Journal of Materials Science*, 56(18), pp. 11098–11113. Available at: https://doi.org/10.1007/s10853-021-05974-3.

Wibowo, A.T. *et al.* (2025) 'Analysis of Variation in the Number of Layers in the Hardfacing Process of ASTM A216 WCB Material on Hardness, Wear, and Microstructure', *PENA TEKNIK: Jurnal Ilmiah Ilmu-Ilmu Teknik*, 10(2), pp. 106–115. Available at: https://doi.org/10.51557/yknegr07.

Zhang, H. *et al.* (2022) 'Effects of Quenching and Tempering Heat Treatment Processing on the Microstructure and Properties of High-Strength Hull Steel', *Metals*, 12(6), p. 914. Available at: https://doi.org/10.3390/met12060914.